AIAA Fluid Dynamics and Co-located Conferences and Exhibit
24 - 27 June 2013
San Diego, California

Statistical inverse analysis and stochastic modeling of transition

G. Serino*, F. Pinna†, P. Rambaud‡and T. E. Magin§
von Karman Institute for Fluid Dynamics, Chausse de Waterloo 72, B-1640 Rhode-St-Genese, Belgium

A computational method is introduced to infer statistical information on laminar to turbulent transition in hypersonic regime. A probabilistic approach is combined to deterministic simulations to take into account the physical variability of the environment and to treat transition as a stochastic mechanism. The input uncertainty is the perturbation spectrum in term of frequency distribution inside the boundary layer upstream of the transition onset. The analysis is divided into a forward and into an inverse problem. In the forward problem, this distribution is first imposed to match experimental data collected in the VKI-H3 hypersonic facility. The transition location is determined in the deterministic simulations with the e^N prediction method which relies on Linear Stability Theory. In the experiments, the transition onset is highlighted by a steep rise of the heat flux measured at the surface of the model. Then, in the inverse problem, the experimental data are used to infer the distribution of the frequency through a Markov-Chain Monte Carlo Method. The approach has demonstrated encouraging results even though further investigation is necessary for a deeper comparison with the experimental data.

Nomenclature

Symbols

A_0	initial amplitude of the disturbances
F	dimensional frequency (kHz)
M	Mach number
N	amplification ratio
N_{crit}	critical N for transition onset
Re	Reynolds number
St	Stanton number
p_T	probability of transition
$\hat{v}(y)$	amplitude of the perturbations
x	streamwise coordinate (m)
y	normal coordinate (m)
z	spanwise coordinate (m)

Greek Symbols

α	streamwise wave number
β	spanwise wave number

*PhD. Candidate, Aeronautics and Aerospace Department, gennaro.serino@vki.ac.be
†Research Engineer, Aeronautics and Aerospace Department, fabio.pinna@vki.ac.be
‡Associate Professor, Aeronautics and Aerospace Department, patrick.rambaud@vki.ac.be
§Assistant Professor, Aeronautics and Aerospace Department, thierry.magin@vki.ac.be

δ_{μ_F}	MCMC increment for the mean
δ_{σ_F}	MCMC increment for the variance
γ	intermittency factor
μ	mean
ω	non-dimensional frequency
σ	variance

Abbreviation

CFD	Computational Fluid Dynamics
DNS	Direct Numerical Simulations
$MCMC$	Markov chain Monte Carlo
QoI	Quantity of Interest
$RANS$	Reynolds Averaged Navier-Stokes
TPS	Thermal Protection System
UQ	Uncertainty Quantification
VKI	von Karman Institute for Fluid Dynamics
cdf	cumulative distribution function
pdf	probability distribution function

I. Introduction

The knowledge of the location of laminar to turbulent transition is essential for numerous engineering applications. For a hypersonic vehicle, an accurate prediction of the transition onset may allow to precisely define the dimensions of the thermal protection system (TPS). The transition onset depends on a large number of parameters and consequently it is difficult to predict. In particular, perturbations in the boundary layer upstream of the transition onset are known to affect this mechanism.

The laminar-turbulent transition process may be divided into three stages: receptivity, linear disturbance evolution, and nonlinear breakdown to turbulence. Most transition modeling approaches are deterministic and rely on empirical data (Menter[10]), but they do not capture the stochastic nature of the physical processes active during these stages. Only the nonlinear breakdown stage, including the formation of turbulent spots, has been modeled in a probabilistic way (Vinod,[27] Pecnick[21]).

Investigations with explicitly forced, controlled perturbations (Marxen[17]) at low levels of free stream turbulence are useful to advance our understanding of mechanisms involved in the laminar-turbulent transition process. These studies consider the so-called controlled deterministic transition. Using random forcing to introduce the disturbances responsible for transition is an alternative to account for the its non-deterministic nature (Marxen[18]). The corresponding process, controlled random transition, is essentially the same as the controlled deterministic transition, except that the forcing is not deterministic.

Natural transition is when intentional forcing of boundary-layer perturbations is entirely absent and the flow still becomes turbulent. In environments with low disturbance levels representative of free flight in the atmosphere, controlled and natural transition share a central feature. The transition process is typically governed by the convective amplification of high-frequency boundary-layer disturbances. Unlike for controlled transition, a commonly accepted way to numerically treat natural transition has not yet emerged. One way to compute natural transition is to apply the numerical approach used for controlled random transition, but with the controlled forcing adapted to the operating conditions of interest (Jacobs[9]).

Such an approach requires a good a priori statistical characterization of the natural disturbance spectrum upstream of the transition location, i.e. a statistical description of frequencies, wave lengths, amplitudes, and relative phase differences. Unfortunately, boundary-layer perturbations are difficult to measure and are usually not sufficiently well characterized experimentally. On the other hand, the region of laminar-turbulent transition is often fairly well documented in the form of skin-friction coefficients or heat transfer at the wall. Our objective is to evaluate whether a statistical inverse analysis, using e.g. measured heat-transfer coefficients as a basis, offers the possibility to provide a characterization of relevant disturbance spectra upstream of the transition zone.

II. Transition modeling and Linear Stability Theory

Todays State-of-the-Art transition models provide a deterministic, fixed transition location.
Two commonly used classes of methods are correlation-based methods and the e^N-method. Correlation-based methods rely on tuning relevant parameters in order to match available experimental data (Serino[24]). On the other hand, Linear Stability Theory (LST) for compressible boundary layers (Mack[11]) is an accurate way to capture the stage of linear disturbance evolution by computing the local growth rate of boundary layer perturbations. It is based on the linearized Navier-Stokes equations together with a parallel-flow assumption. The e^N-method applied to supersonic boundary layers (Malik[14]), considers the integrally most amplified disturbance from LST to yield the transition onset location. Typical N-factors at transition onset lie in the range of $5-10$ (Malik[15]).
Both the receptivity and the nonlinear stages are only indirectly considered in the e^N method by choosing a so-called critical value for N. This value, N_{crit}, hence collectively represents the physical mechanisms active in the receptivity and nonlinear stages. In setups with a high level of freestream turbulence or significant surface roughness, the level of boundary layer perturbations at the end of the receptivity stage is expected to be high. This is reflected by choosing a small N_{crit}. Regarding the nonlinear stage, the standard e^N-method assumes that transition is caused by the linear disturbance which is integrally most amplified and reaches the critical N-factor first, independent of the underlying amplification mechanism.

III. Theoretical background

The probabilistic approach used in the current work can be divided in a forward problem and in an inverse problem. In the forward problem we aim at matching the experimental data by imposing a distribution for the input parameters (e.g. the frequency distribution).In the inverse problem instead, the goal is to find the distribution of the input parameters starting from the experimental data.

A. The forward problem

We assume that laminar-turbulent transition is caused by perturbations in the boundary layer upstream of the transition location. These perturbations often occur in the form of wave packets. In order to better characterize them, a signal g measured somewhere inside the boundary layer at the streamwise location x_0 can be decomposed into J Fourier modes with frequency F, amplitude A_0 and phase ϕ, respectively (here, g can be e.g. a velocity component, temperature, or pressure):

$$g(t) = \sum_{j=1}^{J} A_0^j sin(2\pi F^j t - \phi^j) \tag{1}$$

The signal possesses a random character, i.e. $g(t)$ is a random function, since every measured signal containing one or more wave packets will be slightly different. Below, we consider only a single wave (and neglect phases ϕ):

$$b(t) = A_0 sin(2\pi F t) \tag{2}$$

Both F and A_0 are random variables so that we can define a joint probability density function $PDF(A_0, F)$ and, for instance, $p(A \leq A_c)$ denoting the probability that A is smaller or equal to A_crit, which is the critical amplitude at the transition onset. Below we assume for simplicity a multivariate Gaussian distribution with mean (μ_{A_0}, μ_F), variance (σ_{A_0}, σ_F) and covariance λ.
Downstream of x_0, the amplitude of the wave grows due to a linear instability of the boundary layer. LST can be used to compute the amplitude further downstream $A(x > x_0)$ as a function of the perturbation frequency F. LST yields local amplification rates $\alpha_i(x, F)$ and here we relate the amplitude $A(x)$ to the initial amplitude A_0 as follows:

$$A = A_0 \times \int_{x_0}^{x} max(-\alpha_i(\tilde{x}, F), 0) d\tilde{x} \equiv C_{LST}(x, F) \times A_0 \tag{3}$$

Furthermore, we assume that transition to turbulence occurs at the streamwise location x_T where the amplitude exceeds a critical value $A(x_T) = A_{crit}$. Hence, the probability of having turbulent flow at a given x is defined as follows:

$$p_T(x) = \int_F \int_{A_0} p(A(x, A_0, F) > A_{crit}) dA_0 dF \tag{4}$$

The probability p_T is not measurable experimentally in the transition region. It is more convenient to describe the state of the flow in this region by the intermittency factor γ. This factor specifies the normalized fraction of time for which the flow is turbulent at a given streamwise location. For $\gamma = 0$ the flow is fully laminar and for $\gamma = 1$ it is fully turbulent. We assume that at a given moment in time, transition at the streamwise location x_T causes a steep rise in the wall heat flux Q_w and associated instantaneous Stanton number:

$$St^* = Q_w/(\rho_\infty U_\infty (h_0 - h_w)) \tag{5}$$

where h_0 and h_w are the total enthalpy and the enthalpy at the wall. We assume that the instantaneous Stanton number may possess two different values:

$$St^* = St_{laminar} \quad x < x_T; \quad St^* = St_{turbulent} \quad x \geq x_T \tag{6}$$

Then, γ can be computed from time-averaged measurements of the heat flux and corresponding Stanton number ($St = \bar{St^*}$):

$$\gamma(x) = (St(x) - St_{laminar})/(St_{turbulent} - St_{laminar}) \tag{7}$$

For very long times during which several wave packets have passed the transition region, the intermittency can be assumed to be equal to the probability of the flow to be turbulent, i.e. $p_T(x) = \gamma(x)$. In summary, our forward model serves to connect the measurement of boundary-layer perturbations, the joint probability $PDF(A_0, F)$, with the probability of transition p_T or intermittency γ, with LST lying at the core of the model.

In the application on the experimental data, the forward model is simplified by assuming a single constant (deterministic) A_0 so that the input probability density function is a function of frequency only $PDF(F)$ at x_0. A Gaussian distribution with mean μ_F and variance σ_F is assumed. In this case, instead of using the amplitude A, we use the N-factor as in the e^N-method. It is expressed as an amplitude ratio:

$$N(x, F) = ln(A(x, F)/A_0) \tag{8}$$

Analogously, we replace the critical amplitude A_{crit} by a critical N-factor:

$$N_{crit} = ln(A_{crit}/A_0) \tag{9}$$

For a fixed $x = x^*$, the transfer function $N = N(x^*, F)$ is invertible within the interval $N \in [0, N_{max}]$, and hence the $PDF(N)$ can be computed as:

$$J(F, N) = dF/dN, \quad PDF(N) = J(F, N) \times PDF(F) \tag{10}$$

Integrating along N up to N_{crit} yields:

$$p_T = 1 - \int_0^{N_{crit}} PDF(\tilde{N}) d\tilde{N} = \gamma \tag{11}$$

First results obtained using this simplified model can be found in *Serino et al.*[23] and in *Marxen et al.*[19]. The different steps used in the forward model are presented as follows.

- Definition of the uncertainties: LST has been carried out by considering the variation of the dimensional frequency (F) of the free stream perturbations. The UQ approach aims at defining how the variation of this parameter affects the transition onset location. In order to do that, a probability function (*pdf*) with a normal distribution is assumed to describe this source of uncertainty. Generally, a normal distribution includes all the possible values of a parameters from $-\infty$ to $+\infty$. In the current work,

in order to prevent non physical values, such as negative frequencies, the probability distribution has been truncated into a fixed range. Frequencies are then selected in this range that includes the typical values for *second mode* instability. An example of the *pdf* for the input uncertainties is shown in Fig. 1.

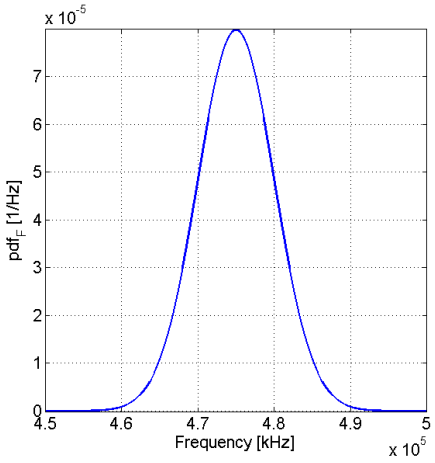

Figure 1. Example of *pdf* of the input parameter for the UQ analysis

- Propagation: LST analysis defines a *transfer function* which links the input uncertainty (i.e. the frequency F) to the output (i.e. the N-factor) for the estimation of the transition onset in the simulations. Once the input *pdf* is assumed, the output *pdf* is obtained by applying the *method of transformation*. This method is valid as long as the $input - output$ relation is unique, that is when the *transfer function* is monotonic. An illustration of the method is represented in Fig. 2 for generic input, $f(x)$, and transfer function $y(x)$. In our case, the *transfer function* $N = N(F)$ is unique up to the maximum N-factor for each curve which describes the relation between the input frequency F and the output N-factor. The method consists in obtaining the output *pdf* by multiplying the input *pdf* and the *Jacobian*, $J(F, N) = dF/dN$, of the *transfer function* as reported in Eq. 10.

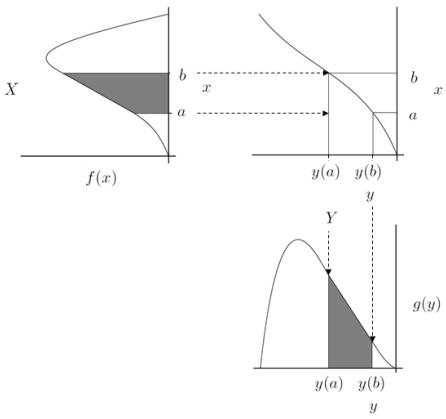

Figure 2. Example of the *method of transformation*

- Output: the probability distribution of the $N-$factor for each station of the computational domain is the output of the analysis. Since the work aims at modeling the transition region, results are presented in terms of the probability of having transition at a fixed location. This probability is computed by integrating, at a fixed streamwise coordinate, along N up to N_{crit}, which is the N value corresponding to the transition onset experimentally observed. The integration is reported in Eq. 11.
The probability of transition starts from 0 where the flow is most likely to be laminar. Then it gradually rises to 1 where the flow is most likely to be fully turbulent. This probability can be interpreted as the

intermittency factor γ, which has been defined by Narasihma[20] as the time ratio between turbulent and laminar flow at a fixed location. A summary of the procedure described above is reported in Fig. 3(a), while in Fig. 3(b) an example of the output probability of transition is shown.

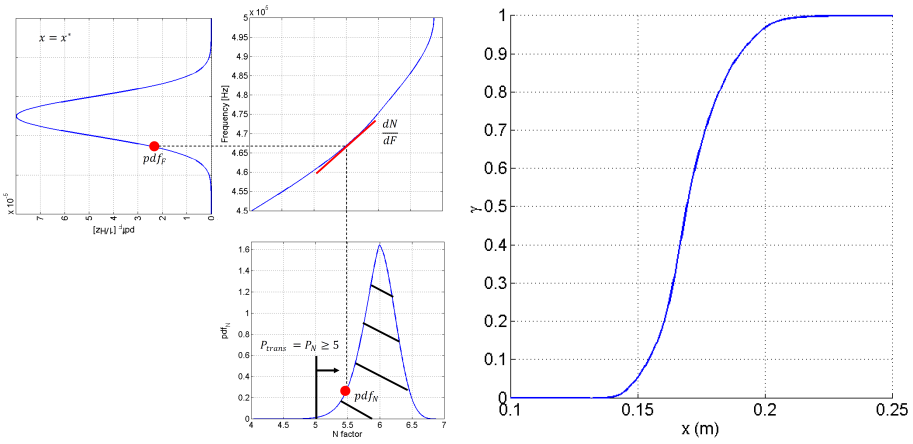

(a) (b)

Figure 3. (a) Summary of the procedure to obtain the probability of transition, (b) Example of probability of transition.

B. The inverse problem

The forward problem described above can be regarded as a computational model $f(s)$ that takes D input parameters $s = (s_1, ..., s_D)$ and produces a K-vector of derived outputs $m = (g_1(f(s), r), ..., g_K(f(s), r))$ with auxiliary parameters $r = (r_1, ..., r_N)$. Solving for m given s is called the forward problem, while inferring s given the measurements of m is denoted as the inverse problem.
For this test case, the simplified forward model is applied, with the two input parameters $s_1 = \mu_F$ and $s_2 = \mu_F$. Auxiliary parameters r are given in Tab.2. Again, we consider as outputs at selected locations $x_1, ..., x_K$ and hence $m = (1, ..., K)$.

P_∞ [Pa]	T_∞ [K]	ρ_∞ [kg/m^3]	U_∞ [m/s]	Re_∞ [1/m]	T_{wall} [K]
1640.41	59.875	0.09529	931.45	2.28E+07	294.73

Table 1: Free stream conditions (subscript ∞) for the test case.

Due to measurement uncertainties, the input quantity s can only be characterized by its statistics, namely the probability $p(s)$. The solution of the forward problem hence yields a probability $p(m)$. In the inverse problem, the measurements of m are noisy, i.e. the input to the statistical inverse problem is $m + \eta$, where η quantifies the noise.
In the inverse problem, we start with given noisy measurements $m+\eta$ and seek the input parameters s using our computational model $f(s)$. The inverse problem is solved by Bayesian inversion. Instead of calculating s, we compute a probability of s given m, $p(s|m)$, which is the so-called posterior density.
Bayes' theorem states that the conditional probability of the parameters s given the measurements m is equal to the product of the probability of the measurements m given the parameters s, times the ratio between the probabilities of the parameters s and the measurements m:

$$p(s|m) = \frac{p(m|s) \times p(s)}{p(m)} \propto p(m|s) \times p(s) \tag{12}$$

where $p(s)$ is the prior probability density which is related to the information on the input parameters and $p(m|s)$ is the likelihood probability which relates the measurements to the input parameters. Finally, $p(m)$ is simply a normalizing constant that ensures that the product of the likelihood and the prior is a probability density function, which integrates to one.
Several methods are available to infer the posterior probability density, for instance the Markov Chain Monte

Carlo (MCMC) method or the Kalman filtering method (Tarantola[25]). The first includes algorithms for sampling from probability distributions based on building a Markov chain that has the desired distribution as its equilibrium distribution. The state of the chain after a large number of steps is then used as a sample of the desired distribution. The quality of the sample improves as a function of the number of steps. For the current application, the MCMC method has been implemented and used to compute $p(s|m)$ with a Metropolis-Hastings algorithm (Hastings[6]). For simplicity, we assume a Gaussian distribution for $p(s)$. The effect of this assumption will be assessed in future works.

IV. Results on the VKI-H3 test case

Here, a test case for natural transition on a 7° half cone model in the VKI-H3 facility is presented. The test conditions are summarized in Tab. 2 for different Reynolds numbers. Experiments were carried out by Masutti[16] and results are represented in Fig. 4. Transition is detected by surface measurements of the heat flux which is then expressed as the non dimensional Stanton number (St). This number quantifies the ratio of heat transferred to the wall and the heat converted through the boundary layer. From experimental data, it can be seen that the transition onset location moves upstream as the free stream Reynolds number increases.

The analysis is divided in two parts. The first is focused on studying how the uncertainties on the freestream perturbations propagate to the numerical results and on the comparison between the numerical results and the experimental data. In the second part, an inverse analysis is carried out to investigate the distribution of the free stream perturbations which are most likely to cause transition for one of the cases. The first analysis is also defined as *the forward problem* and it follows the steps described in Sec. A. The second part is called the *the inverse problem* and it will be described in the following sections.

Test case	M_∞	Re_∞ [1/m]	T_w [K]
Low Reynolds	6.0	18.0×10^6	294
Medium Reynolds	6.0	22.8×10^6	294
High Reynolds	6.0	27.1×10^6	294

Table 2: Test case and free stream conditions

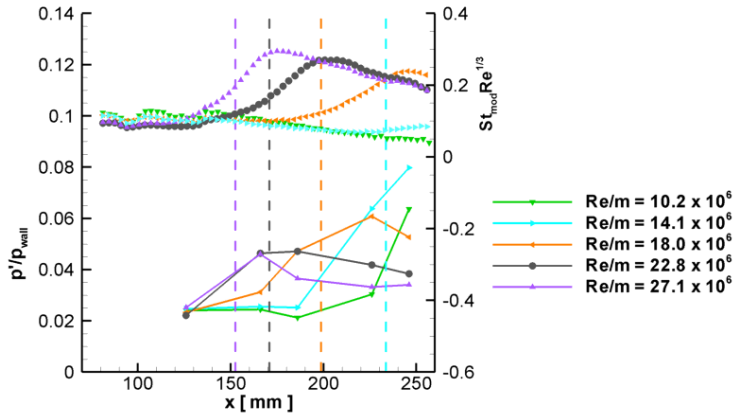

Figure 4. Experimental results obtained in VKI-H3 facility (conditions are given in Tab. 2). Modified Stanton number (top curves) and pressure variations (bottom curves) against the stream wise coordinates

.

A. The forward problem

We assume that laminar-turbulent transition is caused by perturbations in the boundary layer upstream of the transition location. The aim of *the forward problem* is to obtain the probability of transition caused by an assumed free stream perturbation spectrum.
For the conditions indicated in Tab. 2, a linear stability analysis has been carried out and the N-factor has been obtained. Then, a *pdf* has been assumed for the frequencies which characterize the freestream perturbations. We assume that the *pdf* is normally distributed around its mean μ_F with a variance σ_F in a given range of frequencies. The value of the mean and the variance are indicated in Tab. 3 for the different Reynolds numbers. The values have been obtained by choosing the mean of frequency distribution such that the amplification ratio reaches the threshold value at the experimental transition onset. It has been found that, in the VKI-H3 facility, the limiting N-factor is equal to 5. In Fig. 5 the isolines of the N-factor are computed for the High Reynolds conditions in which transition is observed at ≈ 0.13 m (see Fig. 4). A mean frequency of 480 kHz with a variance of 25 kHz allows to have a satisfying agreement with the experimental data.

Test case	μ_f [kHz]	σ_F [kHz]	Range [kHz]
Low Reynolds	330	10	$200 \div 800$
Medium Reynolds	410	20	$200 \div 800$
High Reynolds	480	25	$200 \div 800$

Table 3: Parameters for the input *pdf*

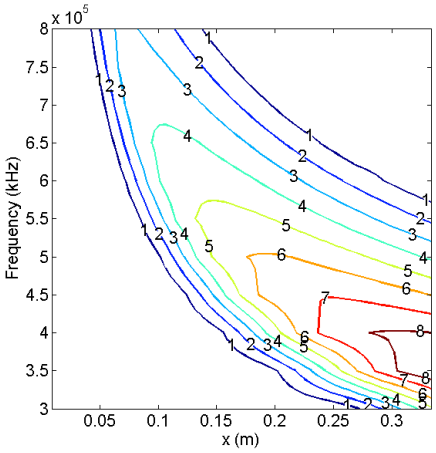

Figure 5. N-factor isolines against Frequency and streamwise coordinate for the High Reynolds condition computed with LST

Experimental data are available in term of Stanton number $St(x)$ (Fig. 4) along the cone model. In order to compare them with our results, the St has been normalized to obtain the experimental intermittency factor γ within the transition region. Since the transition onset x_{onset} and the transition offset x_{offset} are known, the experimental intermittency can be obtained through Eq. 13.

$$\gamma(x) = \frac{St(x) - St_{x=x_{onset}}}{St_{x=x_{offset}} - St_{x=x_{onset}}} \tag{13}$$

The normal distribution with the parameters given in Tab. 3 allows to compute the probability of transition and, thus, the intermittency curves for the different test conditions. Results are represented in Fig. 6 and compared to the experimental data. The transition onset location and the shape of the intermittency factor within the transition region agree very well with the experimental data. For all cases, a characteristic shape is obtained similar to the classical error function. The good agreement with the experimental data demonstrates the validity of the approach and, in particular, confirms the validity of the e^N transition prediction for high-speed flows.

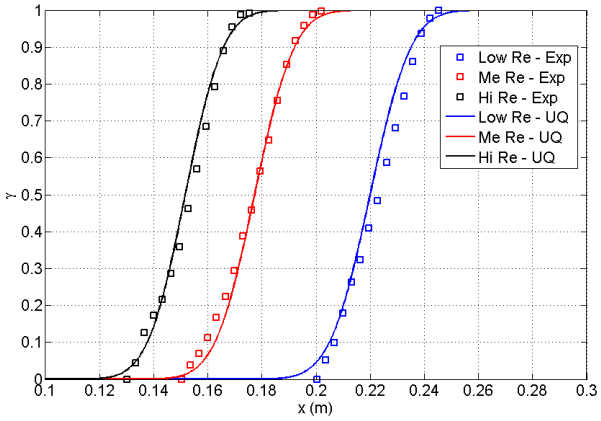

Figure 6. Intermittency as a function of the streamwise location : comparison between UQ analysis (-) and experimental results (□) for the conditions given in Tab. 2.

B. The inverse problem

In our specific context, the inverse problem consists in obtaining the distribution of the frequency which gives the intermittency closest to the experimental data. The parameter to be inferred are the mean μ_F and the variance σ_F of the frequency *pdf* at the transition onset.
This approach has been applied to the VKI-H3 experimental data for the low-Reynolds number case ($Re = 18 \times 10^6$). The inverse problem has been solved by using the Markov-Chain Monte Carlo method where the forward problem is solved several times by varying the input parameters in a given range. Starting from an initial distribution defined by μ_0 and σ_0, successive realizations are obtained with different combinations of the parameters and selected increments (δ_{μ_F}, δ_{σ_F}) for the mean and the variance, respectively. The method guarantees the convergence to the exact solution after a certain number of steps. An illustration of the sampling space is shown in Fig.7 with the starting point (μ_{F0}, σ_{F0}) and the burn in period. The converged mean and variance are evaluated on the remaining samples as represented in Fig.8 and Fig.9. The final values are reported in Tab.4 and compared to the probability distribution previously assumed for the forward problem.

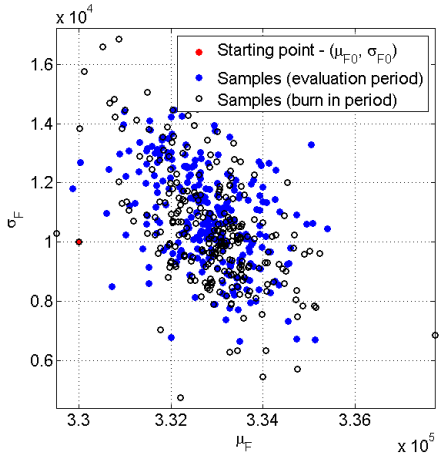

Figure 7. Sampling space : starting point (red), burn in period (black) and useful samples (blue)

The posterior probability density is represented in Fig.10 where it can be seen that the computed intermittency agrees well with the experimental data in the first part of the transition region that is between $0 < P < 0.5$. On the other hand, the agreement is not as good in the second half of the transition region. This is due to the noise η which characterizes the experimental data. The error bars represent the uncer-

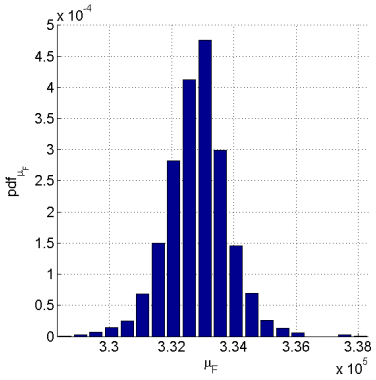

Figure 8. Probability density function for the mean of the frequency (μ_F) for the low Reynolds case

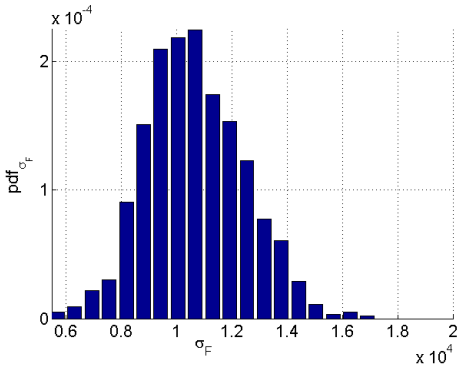

Figure 9. Probability density function for the variance of the frequency (σ_F) for the low Reynolds case

tainty of the measurements, what we called the noise η, which linearly grows in the transitional zone. In fact, when the noise vanishes the agreement is almost perfect as shown for the forward problem (see Fig. 6). For the current case $n = 5000$ samples are used for the MCMC approach which is enough to guarantee the convergence. For the estimation of the steady state, the $Geweke's^4$ test has been used. This consists in splitting the samples in three parts. The first 20% of them represent the "burn-in" period which groups the number of samples necessary to assess the random walk of the MCMC method towards the exact solution. This first percentage is not considered in the final solution. The reamaining samples correspond to the 60% and the 20% of the total. The $Geweke's$ test says that convergence is achieved if the mean of both distributions is approximately the same. In our case, with $n = 5000$ samples the variation on the mean μ_F is 0.1% while the variation on the variance σ_F is 3% between the last two groups of samples.

V. Conclusion

Deterministic tools and a probabilistic approach have been combined to predict laminar to turbulent transition in high speed flows. The method has been applied to experimental data available at the VKI

Low Reynolds	μ_f [kHz]	σ_F [kHz]	Range [kHz]
Forward problem	330	10	$200 \div 800$
Inverse problem	333	11	$200 \div 800$

Table 4: Comparison of the probability density functions for the forward and the inverse problem in the low Reynolds number case

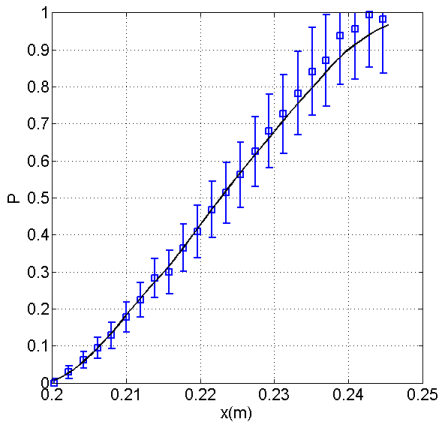

Figure 10. Intermittency as a function of the streamwise location. Comparison of the experimental data with respect to the probability of transition obtained from MCMC.

for laminar transition studies on a cone model. Applications have been presented in terms of the *forward problem* and of the *inverse problem*.
In the *forward problem*, we assumed a distribution for the input uncertainties and, using the e^N transition prediction method, we retrieved the probability of transition or intermittency curve γ. The comparison with experimental data at different Reynolds number has demonstrated the validity of the approach for high speed flows. It should therefore be possible to use the intermittency distributions in order to improve existing transitional models. In fact, in the present case, only the Reynolds number was varied between the different cases but other parameters can vary as well, for example the Mach number. A database of intermittency distribution can be built for different conditions and used to predict transition in numerical simulations. The idea is to use the database validated through comparison with experiments to extrapolate the transition onset in different conditions. In particular, the integration of this approach into existing transitional model for RANS simulations, will be studied in future works.
On the other hand, the *inverse problem* allows to infer disturbance spectra at a location upstream of the transition onset using measured intermittency curves. In the *forward problem*, intermittency curves are computed for a given disturbance spectrum by using LST. The inverse method applies a statistical analysis based on the MCMC method and it has been illustrated using one of the experimentally measured data in the VKI-H3 facility.
For the test case, good agreement was found between the given noisy intermittency curve and the curve resulting from inferred spectra. This suggests that the forward model is able to represent the intermittency curve sufficiently well.
These data will be processed and then used in future works for a better comparison with the results of the inverse analysis. Results could be also improved by using a higher-fidelity forward model since LST lacks in capturing the later stage of the transition process. Moreover, the present method relies on a number of assumptions, including the shape of the *pdf* for the frequency, as well as the kind and number of parameters that are inferred. The effect of these assumptions should carefully be assessed in future works.

Acknowledgment

This research has been financed by the **FRIA-FNRS 2012 fellowship**, annual fellowship of the *Fonds de la Recherche Scientifique* (F.R.S.) for doctoral students.
Results presented in the article has been obtained during the **CTR-Summer Program** 2012 at Stanford University (CA). The author would like to thank Dr. Olaf Marxen, Prof. Gianluca Iaccarino, Dr. Catherine Gorle and Dr. Paul Constantine for their fundamental contribution. A grateful acknowledgment to Dr. Davide Masutti who provided the data on laminar to turbulent transition experiments carried out in the VKI-H3 facility.

References

[1]Arnal D., *Laminar Turbulent Transition Problem in Supersonic and Hypersonic Flows*, ONERA.

[2]Arnal D.,*Special Course on Progress in Transition Modeling*, AGARD report 793, 1993.

[3]Constantine P., *Lectures on Uncertainty Quantification, ME470*, Stanford University, May 2012.

[4]Geweke, J., *Evaluating the Accuracy of Sampling-Based Approaches to the Calculation of Posterior Moments*, Bayesian Statistics 4, Oxford: Oxford University Press, 169-193, 1992

[5]Gorle C., Emory M. and Iaccarino G., *Epistemic uncertainty quantification of RANS modeling for an underexpanded jet in a supersonic cross flow*, Center for Turbulence Research Annual Research Briefs 2011.

[6]W.K. Hastings, *Monte Carlo sampling methods using Markov chains and their applications*, Biometrika 57, 97109, 1970.

[7]Iaccarino G., Eldred M., Doostan A., Ghattas O., *Introduction to Uncertainty Quantification*,SIAM CSE Conference, Miami, FL, 2009.

[8]Iaccarino G., Pettersson P., Nordstr J. & Witteveen J., *Numerical methods for uncertainty propagation in high speed flows*,V European Conference on Computational Fluid Dynamics, ECCOMAS CFD 2011, Lisbon, Portugal, 14-17 June 2010.

[9]Jacobs, R. G. & Durbin, P. A., *Simulations of bypass transition*, J. Fluid Mech.428, 185212, 2001.

[10]Langtry, R. B. & Menter, F. R. *Correlation-Based Transition Modeling for Unstructured Parallelized Computational Fluid Dynamics Codes*, AIAA J. 47 (12), 28942906, 2009.

[11]Mack L. M., *Boundary layer stability theory*, 1969, JPL, Report 900-277.

[12]Mack, L. M., *Linear Stability Theory and the Problem of Supersonic Boundary-Layer Transition*, AIAA Journal., Vol. 13, No.3, pp 278-289, March 1975.

[13]Mack, L. M., *Boundary Layer Linear Stability Theory*, AGARD Report No.70g, June 1984.

[14]Malik M. R., *Instability and transition in supersonic boundary layers*, Energy Sources Technology Conference, New Orleans, LA, February 1984.

[15]Malik, M. R., *Hypersonic flight transition data analysis using parabolized stability equations with chemistry effects*, J. Spacecraft Rockets 40 (3), 332344, 2003.

[16]Masutti D., *Natural and induced transition on a 7° half-cone at Mach 6*, Proceedings of the 2012 VKI PhD. Symposium, von Karman Institute for Fluid Dynamics, 2012.

[17]Marxen O., Iaccarino G. & Shaqfeh E., *Boundary-layer transition via spatially growing oblique waves*, under consideration for publication in Journal of Fluid Mechanics, 2011.

[18]Marxen, O. & Iaccarino, G., *Transitional and turbulent high-speed boundary layers on surfaces with distributed roughness*, AIAA Paper 2009171 pp. 113, 2009.

[19]Marxen, O., Iaccarino, G. & Shaqfeh, E., *Disturbance evolution in a Mach 4.8 boundary layer with two-dimensional roughness-induced separation and shock*, J. Fluid Mech. 648, 435469, 2010.

[20]Narasimha R.,*On the distribution of intermittency in the transition region of a boundary layer*, Journal of Aeronautical Science, vol. 24, pp. 711-712, 1957.

[21]Pecnik R., Witteveen J. & Iaccarino G., *Uncertainty quantification for laminar-turbulent transition prediction in RANS turbomachinery applications*, 49th AIAA Aerospace Sciences Meeting including the New Horizons Forum and Aerospace Exposition, Orlando, Florida, AIAA 2011-660.

[22]Pinna F., *Numerical study of stability of flows from low to high Mach number*, PhD Thesis, von Karman Institute for Fluid Dynamics and Universitá di Roma 'La Sapienza', 2012.

[23]Serino G., Marxen O., Pinna F., Rambaud P. & Magin T., *Transition prediction for oblique breakdown in supersonic boundary layers with uncertain disturbance spectrum*, AIAA 20122973 pp. 111, 2012.

[24]Serino G., Pinna, F. & Rambaud, P., *Numerical computations of hypersonic boundary layer roughness induced transition on a flat plate*, AIAA 20120568 pp. 116., 2012.

[25]Tarantola A., *Inverse problem theory and methods for model parameters estimation*, Siam, 1987.

[26]van Ingen J.L., *The eN method for transition prediction : Historical review of work at TU Delft*, 38th Fluid Dynamics Conference and Exhibit, 23 - 26 June 2008, Seattle, Washington.

[27]Vinod N. & Govindarajan, R., *Pattern of breakdown of laminar flow into turbulent spots*, Phys. Rev. Lett. 93 (11), 114501, 2004.